# Double-resonance optical-pumping effect and ladder-type electromagnetically induced transparency signal without Doppler background in cesium atomic vapour cell



2011 Chinese Phys. B 20 044202

(http://iopscience.iop.org/1674-1056/20/4/044202)

Chin. Phys. B Vol. 20, No. 4 (2011) 044202

# Double-resonance optical-pumping effect and ladder-type electromagnetically induced transparency signal without Doppler background in cesium atomic vapour cell*

Yang Bao-Dong(杨保东), Gao Jing(高 静), Liang Qiang-Bing(梁强兵), Wang Jie(王 杰), Zhang Tian-Cai(张天才), and Wang Jun-Min(王军民)†

*State Key Laboratory of Quantum Optics and Quantum Optics Devices, and Institute of Opto-Electronics, Shanxi University, Taiyuan* 030006, *China*

(Received 13 August 2010; revised manuscript received 19 September 2010)

In a Doppler-broadened ladder-type cesium atomic system ($6S_{1/2}$–$6P_{3/2}$–$8S_{1/2}$), this paper characterizes electromagnetically induced transparency (EIT) in two different experimental arrangements, and investigates the influence of the double-resonance optical-pumping (DROP) effect on EIT in both arrangements. When the probe laser is weak, DROP is explicitly suppressed. When the probe laser is moderate, population of the intermediate level ($6P_{3/2}$ $F' = 5$) is remarkable, therefore DROP is mixed with EIT. An interesting bimodal spectrum with the broad component due to DROP and the narrow part due to EIT has been clearly observed in cesium $6S_{1/2}$ $F = 4$–$6P_{3/2}$ $F' = 5$–$8S_{1/2}$ $F'' = 4$ transitions.

**Keywords:** electromagnetically induced transparency, double-resonance optical pumping, laser spectroscopy

**PACS:** 42.50.Gy, 32.80.Xx, 42.62.Fi **DOI:** 10.1088/1674-1056/20/4/044202

## 1. Introduction

The electromagnetically induced transparency (EIT)[1,2] is a kind of destruction-interference atomic coherence effect, and it can dramatically modify the characteristics of atomic gas, which is initially opaque but can be changed to nearly transparent to a probe laser when a strong coupling laser exists. Accompanied with this absorption reduction, the dispersion will abruptly change and yield the result that the group velocity of the optical pulse amazingly decreases (slow light),[3] or even stops completely[4,5] inside the atomic gas. In recent decades, the EIT effect has attracted considerable attention because it has promising potential applications in quantum memory[6−8] and quantum repeaters[9] in quantum information processing, quantum metrology,[10] Rydberg atomic state detection,[11,12] and so on.

The formation of a coherent superposition dark state, which is not coupled to both the probe and the coupling lasers, is responsible for absorption reduction in EIT. Λ-type three-level system quantum coherence between two ground states (hyperfine levels or Zeeman sublevels) plays a role in the formation of a coherent superposition dark state,[1,2] but for a ladder-type three-level system that is coherence between the ground state and upper excited state.[13] Actually, in the above-mentioned atomic system, EIT is often in company with the optical pumping effect, which also modifies absorption of the probe beam via the change in population on relevant energy levels.[14−18] Recently, Ye *et al.*[14] studied the influence of optical pumping by the coupling laser on the EIT signal in a Λ-type atomic system. Jiang *et al.*[16] investigated enhancement of the EIT signal by an additional optical pumping field.

In the ladder-type cesium atomic system $6S_{1/2}$–$6P_{3/2}$–$8S_{1/2}$ (Fig. 1), we note that two kinds of optical pumping effect, single-resonance optical pumping (SROP) and the double-resonance optical pumping (DROP), should be considered. Although the frequency of the probe laser is locked to the $F = 4$–$F' = 5$ transition, SROP will still transfer the partial population of the $F = 4$ to the $F = 3$ level via

*Project partially supported by the National Natural Science Foundation of China (Grant Nos. 61078051, 60978017, 10974125 and 60821004), the NCET Project from the Education Ministry of China (Grant No. NCET-07-0524), the Specialized Research Fund for the Doctoral Program of China (Grant No. 20070108003).

†Corresponding author. E-mail: wwjjmm@sxu.edu.cn



*http://www.iop.org/journals/cpb http://cpb.iphy.ac.cn*

$F=4$–$F'=3(4)$ excitations and the $F'=3(4)$–$F=3$ decay channel because the energy space between the hyperfine levels in $6P_{3/2}$ is within the Doppler width; simultaneously, DROP will also transfer the partial population of the $F=4$ to the $F=3$ level via $F=4$–$F'=5$–$F''=4$ two-step excitation and the $F''=4$–$F'=3(4)$–$F=3$ and $F''=4$–$7P_{1/2}(7P_{3/2})$–$F=3$ decay channels. The SROP and DROP result in reduction of the population on the $F=4$ level, they will reduce the probe beam's absorption like EIT, and will be mixed with EIT so that it is difficult to distinguish them in experiments. In this paper, we present our experimental investigation on the influence of the DROP effect on EIT in a Doppler-broadened ladder-type cesium atomic system ($6S_{1/2}F=4$–$6P_{3/2}F'=5$–$8S_{1/2}F''=4$) in two different arrangements. We have clearly observed an interesting bimodal spectrum in which the broad component is due to DROP and the narrow part is due to EIT.

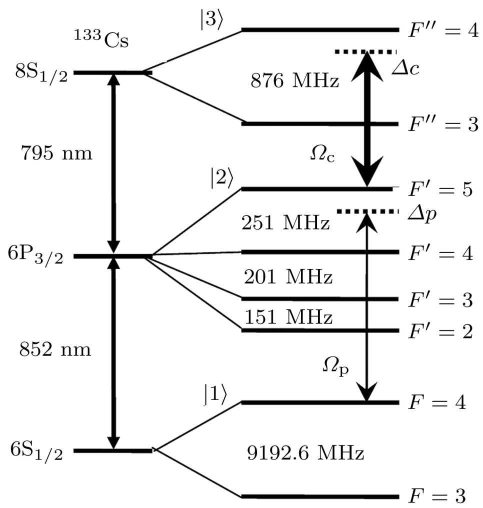


**Fig. 1.** Relevant energy levels of cesium atoms. The $\Delta_p$ and $\Omega_p$ are the frequency detuning and the Rabi frequency of the probe laser, respectively, while $\Delta_c$ and $\Omega_c$ are the frequency detuning and the Rabi frequency of the coupling laser, respectively.

## 2. Experimental setup

The relevant energy levels of cesium atoms are depicted in Fig. 1. Our three-level ladder-type atomic system consists of the hyperfine levels labeled $|1\rangle$, $|2\rangle$ and $|3\rangle$. The spontaneous decay rate from the $6P_{3/2}$ to the $6S_{1/2}$ state is $\Gamma_{21}/2\pi = 5.22$ MHz, and that from the $8S_{1/2}$ to the $6P_{3/2}$ state is $\Gamma_{32}/2\pi = 2.18$ MHz. The $F=4$–$F'=5$ ($|1\rangle$–$|2\rangle$) cycling transition is driven by the probe laser with Rabi frequency $\Omega_p$ and frequency detuning $\Delta_p$, while the $F'=5$–$F''=4$ ($|2\rangle$–$|3\rangle$) hyperfine transition is coupled by the coupling laser with the Rabi frequency $\Omega_c$ and frequency detuning $\Delta_c$.

For a Doppler-broadened ladder-type atomic system, if the probe and coupling lasers take co-propagating configuration inside the vapour cell, the atomic coherence will be mostly submerged by the Doppler effect, so the EIT signal is very difficult to observe unless the Rabi frequency of the coupling laser $\Omega_c$ is bigger than the Doppler broadening $\Delta\omega_D$ ($\Omega_c > \Delta\omega_D$). This is one needs a more intense coupling laser to observe ladder-type EIT in the earlier experiment.[19] If the probe and coupling lasers take the counter-propagating (CTP) configuration, the Doppler effect will be almost eliminated if the $\omega_p \sim \omega_c$ (cesium $6S_{1/2}$ $F$=4–$6P_{3/2}$ $F'=5$–$8S_{1/2}$ $F''=4$ ladder-type system can meet this demand), because the CTP configuration is two-photon Doppler-free in the ladder-type atomic system.[13] In this case, the ladder-type EIT only requires $\Omega_c > (\Delta\omega_D \times \Gamma_{32}/2)^{1/2}$, and $\Gamma_{32}$ is often much smaller than $\Delta\omega_D$, so $\Omega_c$ can be much smaller than $\Delta\omega_D$. Briefly, ladder-type EIT experiments in the CTP configuration do not need an intense coupling laser anymore,[13] so we adopt the CTP configuration in our experiment.

A schematic diagram of the experimental setup is shown in Fig. 2. A commercial grating-feedback

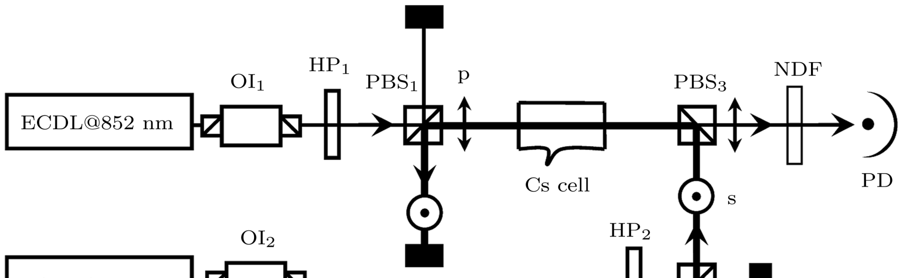


**Fig. 2.** Schematic diagram of experimental setup. The keys to figure: ECDL: external-cavity diode laser; OIs: optical isolators; HPs: half-wave plates; PBS: broad-band polarization beam splitter cube; p: p polarization; s: s polarization; NDF: neutral density filter plate; PD: photodiode.

external-cavity diode laser (ECDL) at 795 nm (Toptica DL-100L) with typical line-width of ~500 kHz (in 50 ms) is used as the coupling laser, while a home-made ECDL at 852 nm with roughly the same line-width serves as the probe laser. The conventional frequency modulation technique for a saturated absorption profile is adopted to lock the probe laser to an $F = 4$–$F' = 5$ cycling transition (this part is not shown in Fig. 2).

After passing an optical isolator (Isowave, Model I-80T-5L) with a typical isolation of > 40 dB, the optical power of the probe and coupling lasers can be adjusted conveniently by corresponding sets of modules consisting of a half-wave plate (HP) and a polarization beam splitter (PBS) cube. Then the probe and coupling laser beams are arranged to counter-propagate with orthogonal linear polarizations passing through a cesium vapour cell (~ ϕ25 mm × 50 mm) at room temperature. The beams with a diameter of $\phi_{\rm p} \sim 2.0$ mm for the probe beam and $\phi_{\rm c} \sim 2.2$ mm for the coupling beam are overlapped inside the cesium vapour cell. Two PBS cubes are used to combine and separate the two beams. The probe laser's transmission signal is collected by a photodiode (New Focus, Model 2001) and displayed on a digital storage oscilloscope (not shown in Fig. 2). A confocal Fabry–Perot cavity (not shown in Fig. 2) with finesse of ~100 and a calibrated free spectra range of 503 MHz is used for measurement of the line-width of EIT signal.

## 3. Experimental results and discussion

### 3.1. Ladder-type EIT signals in two different arrangements

To obtain a nearly pure EIT signal in a ladder-type atomic system as shown in Fig. 1, we have to greatly suppress the SROP effect, and the $F = 4$–$F' = 5$ closed cycling transition is selected for the probe laser. Further to suppress the DROP effect, a weak probe beam ($\Omega_{\rm p} < \Gamma_{21}$) should be adopted so that the population of the $F' = 5$ level is not remarkable. Under these conditions, the other hyperfine levels ($6{\rm S}_{1/2}F = 3$, $6{\rm P}_{3/2}$ $F' = 3$ and $F' = 4$) which do not directly interact with the coupling and probe lasers are neglected approximately in the ladder-type three-level model ($6{\rm S}_{1/2}F = 4$–$6{\rm P}_{3/2}$ $F' = 5$–$8{\rm S}_{1/2}$ $F'' = 4$). In our experiment, the probe beam's power is set to ~23 μW, yielding $\Omega_{\rm p}/2\pi \sim 3$ MHz $< \Gamma_{21}/2\pi$ to avoid remarkable population on the $F' = 5$ hyperfine level for effectively suppressing the DROP effect.

The EIT is substantially interpreted that the atoms are prepared in a dark superposition state of the ground state $|1\rangle$ and higher excited state $|3\rangle$ for the ladder-type system, so EIT under the following two arrangements in the case of the CTP configuration has the same physical nature and different EIT signal profiles.

In the arrangement #1, the coupling laser (~1.6 mW, $\Omega_{\rm c}/2\pi \sim 13.4$ MHz) is fixed on resonance with $F' = 5$–$F'' = 4$ transition ($\varDelta_{\rm c} \sim 0$) while the probe laser is scanned over $F = 4$–$F' = 3$, 4, and 5 transitions, and the spectral profile is the same with the traditional EIT accompanied by a Doppler background, as shown in Fig. 3(a). If the coupling laser is detuned to an $F' = 5$–$F'' = 4$ transition ($\varDelta_{\rm c} \neq 0$), EIT peak will appear at the position where the two-photon detuning $\varDelta = \varDelta_{\rm c} + \varDelta_{\rm p}$ is zero. These results have been demonstrated in previous ladder-type EIT experiments.[13]

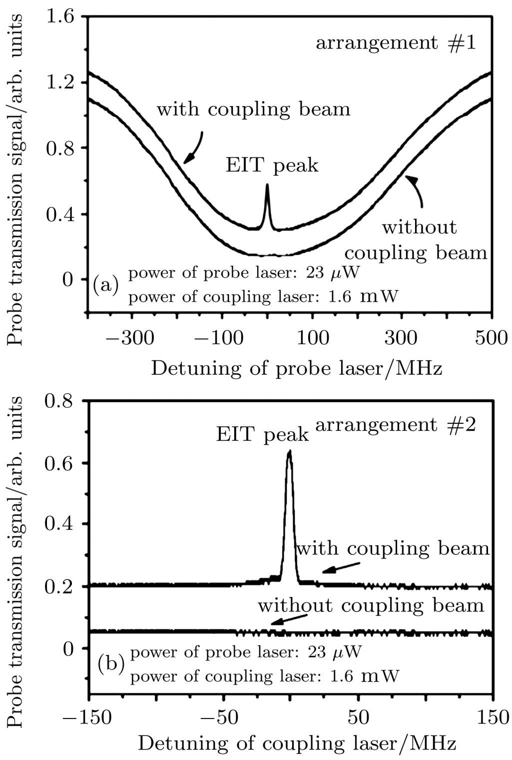


**Fig. 3.** Typical ladder-type EIT signals. (a) The arrangement #1 in which the coupling laser is resonant with $F' = 5$–$F'' = 4$ transition ($\varDelta_{\rm c} \sim 0$) while the probe laser is scanned over $F = 4$–$F' = 3$, 4, and 5 transitions. (b) The arrangement #2 in which the coupling laser is scanned over the $F' = 5$–$F'' = 4$ transition while the probe laser is locked to the $F = 4$–$F' = 5$ cycling transition ($\varDelta_{\rm p} \sim 0$). The $\Omega_{\rm p}/2\pi \sim 3$ MHz, $\Omega_{\rm c}/2\pi \sim 13.4$ MHz. The up-down shifts of traces with and without the coupling beam do not mean a change in transmission background and are just for convenient comparison.

However, in arrangement #2, the coupling laser is scanned over the $F' = 5$–$F'' = 4$ transition while the probe laser is locked to the $F = 4$–$F' = 5$ cycling transition ($\Delta_{\rm p} \sim 0$). Compared with Fig. 3(a), a distinctly characteristic, no Doppler background is observed in both cases with and without the coupling beam, thanks to the velocity-selective mechanism by the frequency-locked probe laser, as shown in Fig. 3(b). The EIT peak appears at the exact position where the coupling laser is resonant with the $F' = 5$–$F'' = 4$ transition. Such a profile of the EIT without a Doppler background may be more suitable for the application of laser frequency stabilization, the investigation of high-resolution spectroscopy and so on.

Here, we will pay more attention to the EIT signals in arrangement #2. The probe beam's power is still set to $\sim 23$ μW ($\Omega_{\rm p}/2\pi \sim 3$ MHz$< \Gamma_{21}/2\pi$), and the coupling beam's power is varied from 0.025 mW to 0.6 mW ($\Omega_{\rm c}/2\pi : 1.67$ MHz $\sim 8.2$ MHz), the magnitude of the EIT peaks in the arrangement #2 is measured. The magnitude of the EIT signal is nonlinearly enhanced with the increasing coupling beam's intensity, and then tends to saturate, and similar results have been obtained in Refs. [13] and [20] based on this arrangement #1.

Now we consider the line-width of the EIT signals in arrangement #2. Obviously, the line-width of the coupling and probe lasers as well as the mutual phase coherence between the two lasers will take effect to the line-width of EIT signal. The lasers with a narrower line-width and good mutual phase coherence by relative phase locking are desired for obtaining a narrower EIT peak. Collisions between atoms and between atoms and the internal wall of the vapour cell will partially destroy the atomic coherence, and therefore will broaden the line-width of the EIT signal. So people usually use an atomic vapour cell filled with buffer gas with the correct partial pressure[21] or a paraffin coated atomic vapour cell[22] to keep the atomic coherence. In our experiment, two grating-feedback ECDLs with typical line-widths of $\sim 500$ kHz are used as the coupling and probe lasers. However, we did not concern the mutual phase coherence and also did not use a buffer gas filled or paraffin coated cesium vapour cell. The influence of the coupling laser's intensity on the line-width of the EIT peak is also investigated. When the coupling beam's power is varied from 0.025 mW to 0.6 mW ($\Omega_{\rm c}/2\pi : 1.67$ MHz $\sim 8.2$ MHz), the line-width of the EIT peak is measured by using a confocal Fabry–Perot cavity. The results are presented in Fig. 4 (the upper trace). The line-width of the EIT peak is roughly kept at $\sim 6.8$ MHz within the measuring error range, which is close to the natural line-width of the $6{\rm P}_{3/2}$ state ($\Delta\nu_{21} = 5.22$ MHz). Here, we have to clarify that the line-width of the EIT peak should increase as the power of the coupling laser increases. However, due to the Doppler averaging effect in the room-temperature vapour cell,[23] the increase in the EIT peak's line-with is so slow that the increasing trend is almost submerged by the measurement error. For a stronger coupling beam, e.g., the coupling power increases up to $\sim 61.7$ mW ($\Omega_{\rm c}/2\pi \sim 83$ MHz), the line-width is measured to $\Delta\nu \sim 11.6$ MHz for $\Omega_{\rm p}/2\pi \sim 2.1$ MHz ($\sim 11.1$ μW of the probe beam, the lowest trace in Fig. 5(b)), and it is only slightly broadened. Similar results have also reported in recent EIT experiments based upon arrangement #1.[23]

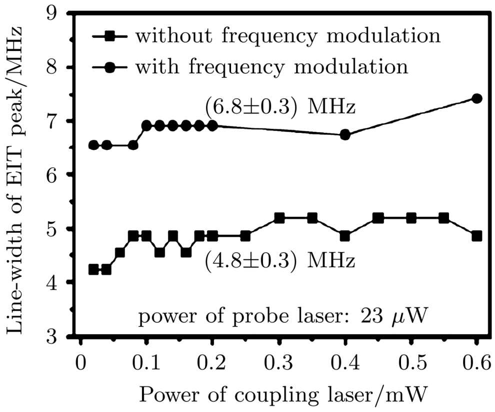


**Fig. 4.** The comparison of the line-width of the EIT peak in arrangement #2 when the probe laser is locked to the $F = 4$–$F' = 5$ cycling transition by a saturated absorption spectroscopic scheme with frequency modulation and a modulation-free polarization spectroscopic scheme, respectively. The solid lines are to guide the eyes.

We have proved that another important factor influencing the line-width of the EIT peak is the frequency stability of the probe laser. The lower the frequency stability of the probe laser, the wider the velocity distribution range of the atoms populated in the intermediate state $F' = 5$ due to the Doppler effect, therefore the broader the EIT peak due to residual DROP effect. This point is demonstrated in our experiment. When the probe laser with a fixed power of $\sim 23$ μW ($\Omega_{\rm p}/2\pi \sim 3$ MHz$< \Gamma_{21}/2\pi$) is locked to the $F = 4$–$F' = 5$ cycling transition by saturated absorption with frequency modulation, the average line-width of the EIT peak for coupling laser's power changed from 0.02 mW to 0.60 mW ($\Omega_{\rm c}/2\pi : 1.5$ MHz $\sim 8.2$ MHz) is (6.8±0.3) MHz, which is clearly broader than the average line-width of $(4.8 \pm 0.3)$ MHz when the probe laser is locked by using the modulation-free polarization spectroscopic technique under the same experimental conditions as shown in Fig. 4. This is because the modulation-free polarization spectroscopic locking technique does not have the extra noise of the probe laser, therefore it can clearly improve the frequency stability, as compared with the case involving the conventional saturation-absorption spectroscopic locking technique.[24]

The above results tell us that the line-width of the EIT signal in arrangement #2 is not observably broadened with the increase in coupling laser's intensity for the Doppler averaging effect.[23] However, its line-width will be greatly broadened with increasing probe laser's intensity for the increasing optical pumping effect (SROP and DROP).

## 3.2. Influence of DROP effect on EIT

Now we will investigate the influence of the DROP effect on the EIT on the basis of cesium $6S_{1/2}$ $F = 4$–$6P_{3/2}$ $F' = 5$–$8S_{1/2}$ $F'' = 4$ transitions. The $F = 4$–$F' = 5$ cycling transition is selected for effectively avoiding the SROP effect. In addition, here the probe beam is not weak ($\Omega_p \geq \Gamma_{21}$), the population on the intermediate state ($6P_{3/2}$ $F' = 5$) is considerable in both arrangements #1 and #2, and so the DROP effect will play a remarkable role, and mix with the EIT in the spectral signal.

For more details in arrangement #1, the atoms with different velocity are partially transferred from the $F = 4$ to the $F' = 5$ level by the scanning probe laser due to the Doppler shift. Among them, the zero-velocity atoms are further partially excited to the $F'' = 4$ level by velocity-selective excitation of the coupling laser, which is fixed on resonance with the $F' = 5$–$F'' = 4$ transition. But in arrangement #2, the two-step excitation is a little bit different from that in arrangement #1. Only the zero-velocity atoms are partially transferred from the $F = 4$ to the $F' = 5$ level by velocity-selective excitation of the probe laser, which is locked to the $F = 4$–$F' = 5$ cycling transition, then when the coupling laser is scanned to the $F' = 5$–$F'' = 4$ transition, some of them are further excited to the $F'' = 4$ level. Finally, these zero-velocity atoms on the $F'' = 4$ level in both arrangements #1 and #2 will decay to the $F = 3$ level via the $F'' = 4$–$F' = 3(4)$–$F = 3$ and $F'' = 4$–$7P_{1/2}(7P_{3/2})$–$F = 3$ decay channels, which will decrease absorption of the probe beam.

When the coupling beam's power is fixed to ∼ 24 mW ($\Omega_c/2\pi \sim 52$ MHz), figure 5(a) presents the transmission signals of the probe beam as a function of the probe laser's detuning with different probe beam's power (73.7 μW ∼ 112.4 μW, corresponding to $\Omega_p/2\pi$ : 5.3 MHz ∼ 6.6 MHz) in arrangement #1. For a more intense coupling beam, for example, when the coupling beam's power is fixed to ∼ 61.7 mW ($\Omega_c/2\pi \sim 83$ MHz), arrangement #2 is adopted and the transmission signals of the probe beam as a function of the coupling laser's detuning with different probe beam's power (11.1 μW ∼ 284.8 μW, corresponding to $\Omega_p/2\pi$ : 2.1 MHz ∼ 10.5 MHz) are presented in Fig. 5(b).

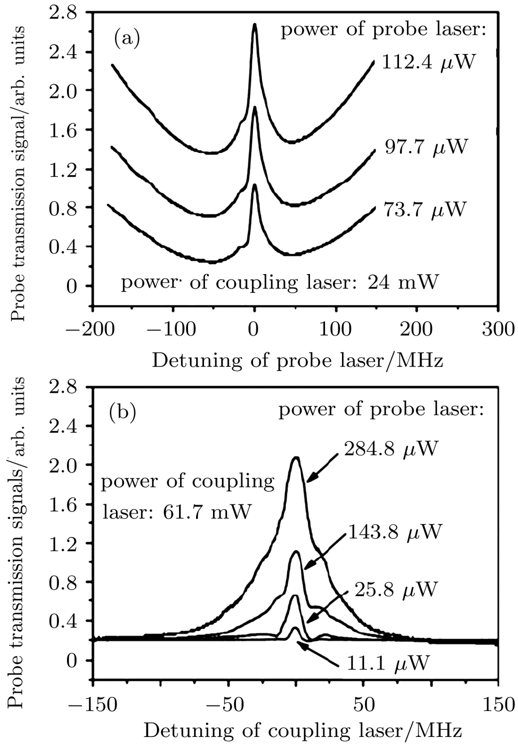


**Fig. 5.** (a) Transmission signals of the scanning probe beam vary as a function of the probe laser's detuning with different probe beam's power but fixed the coupling beam's power to ∼ 24 mW ($\Omega_c/2\pi \sim 52$ MHz) in arrangement #1. The up-down shifts of traces in (a) do not mean a change in transmission background and are just for convenient comparison. (b) Transmission signals of the locked probe beam vary as a function of the coupling laser's detuning with different probe beam's power but fixed the coupling beam's power to ∼ 61.7 mW ($\Omega_c/2\pi \sim 83$ MHz) in the arrangement #2. Clear bimodal spectra are shown in both (a) and (b).

Figures 5(a) and 5(b) clearly show bimodal structures in the transmission spectrum. We ascribe the narrow part on top to the EIT, which is narrower when we particularly consider the Doppler averaging effect.[23] Even $\Omega_c > \Gamma_{21}$, the narrow EIT peak is still indicated as shown in Fig. 4. To a certain extent, the EIT effect suppresses the DROP effect. The broad component on the bottom is due to the DROP effect, which is associated with the spontaneous decay rates ($\Gamma_{32}$ and $\Gamma_{21}$), and is getting much broader along with the increase in the probe beam's intensity. In our experiment, cesium $6S_{1/2}$ $F = 4$–$6P_{3/2}$ $F' = 5$–$8S_{1/2}$ $F'' = 4$ transitions are used, and the spontaneous decay channels ($F'' = 4$–$F' = 3(4)$–$F = 3$ and $F'' = 4$–$7P_{1/2}(7P_{3/2})$–$F = 3$ transitions) with which DROP takes effect are explicitly recognized from the cesium $8S_{1/2}F'' = 4$ level to the $6S_{1/2}$ $F = 3$ level. In particular, the blue fluorescent light at 456 nm and 459 nm can be clearly observed by the naked eye due to $7P_{1/2}(7P_{3/2})$–$6S_{1/2}$ spontaneous decay in the experiment. The weaker the probe beam ($\Omega_p < \Gamma_{21}$), the weaker the blue fluorescent light due to a much lower DROP rate. For another important proof of the DROP effect, we can still observe a peak due to reduction absorption to the probe beam in both arrangements for the co-propagating configuration, but this peak is not an EIT signal according to Refs. [13] and [18]. To theoretically explain this bimodal structure in the transmission spectrum of the probe beam, density-matrix equations considering relevant hyperfine levels in the $6S_{1/2}$, $6P_{3/2}$, $8S_{1/2}$, $7P_{1/2}$, and $7P_{3/2}$ states should be used, so that the EIT and DROP effects are included in the theoretical system.

## 4. Conclusion

In conclusion, ladder-type EIT with cesium $6S_{1/2}$ $F = 4$–$6P_{3/2}$ $F' = 5$–$8S_{1/2}$ $F'' = 4$ transitions has been characterized in two different experimental arrangements, and the influence of DROP on ladder-type EIT has been investigated in both arrangements. When the probe laser is not weak ($\Omega_p \geq \Gamma_{21}$), the DROP effect will play a considerable role since the population of the intermediate state is remarkable. We have observed a bimodal structure in the transmission spectrum, in which the broad component is due to DROP and the narrow part is due to the EIT. When the probe laser is weak ($\Omega_p < \Gamma_{21}$), the DROP effect can be neglected approximately in experiments. The line-width of the EIT peak without a Doppler background in arrangement #2 is not observably broadened with increasing coupling laser's power due to the Doppler averaging effect. In addition, the line-width is narrower when the probe laser is locked by using the modulation-free polarization spectroscopic scheme than in the case using the frequency-modulation saturation absorption spectroscopic scheme. A narrower line-width of $\sim 4.8$ MHz is obtained, which is comparable to the natural line-width of the $6P_{3/2}$ state ($\Delta\nu_{21} = 5.22$ MHz).

We believe that our experimental investigations and results are helpful to understand the EIT and DROP effects in a ladder-type atomic system and their relationship, and also hope to provide some useful references for relevant applications: to detect highly excited Rydberg atomic states,[11,12] to set up a laser frequency standard by using ladder-type EIT or DROP spectroscopy,[25,26] to measure the hyperfine splitting and hyperfine structure constant in the excited state, and so on.

## References

[1] Harris S E 1997 *Phys. Today* **50** 36

[2] Lukin M D and Imamoglu A 2001 *Nature* **413** 273

[3] Hau L V, Harris S E, Dutton Z and Behroozi C H 1999 *Nature* **397** 594

[4] Liu C, Dutton Z, Behroozi C H and Hau L V 2001 *Nature* **409** 490

[5] Phillips D F, Fleischhauer A, Mair A, Walsworth R L and Lukin M D 2001 *Phys. Rev. Lett.* **86** 783

[6] Lvovsky A I, Sanders B C and Tittel W 2009 *Nature Photonics* **3** 706

[7] Zhao B, Chen Y A, Bao X H, Strassel T, Chuu C S, Jin X M, Schmiedmayer J, Yuan Z S, Chen S and Pan J W 2009 *Nature Phys.* **5** 95

[8] Zhao R, Dudin Y O, Jenkins S D, Campbell C J, Matsukevich D N, Kennedy T A B and Kuzmich A 2009 *Nature Phys.* **5** 100

[9] Briegel H J, Dür W, Cirac J I and Zoller P 1998 *Phys. Rev. Lett.* **81** 5932

[10] Banaszek K, Demkowicz-Dobrzański R and Walmsley I A 2009 *Nature Photonics* **3** 673

[11] Mohapatra A K, Jackson T R and Adams C S 2007 *Phys. Rev. Lett.* **98** 113003

[12] Kubler H, Shaffer J P, Baluktsian T, Low R and Pfau T 2010 *Nature Photonics* **4** 112

[13] Gea-Banacloche J, Li Y Q, Jin S Z and Xiao M 1995 *Phys. Rev.* A **51** 576

[14] Ye C Y and Zibrov A S 2002 *Phys. Rev.* A **65** 023806

[15] Chakrabarti S, Pradhan A, Ray B and Ghosh P N 2005 *J. Phys.* B: *At. Mol. Opt. Phys.* **38** 4321

[16] Jiang W, Chen Q F, Zhang Y S and Guo G C 2006 *Phys. Rev.* A **73** 053804

[17] Moon H S, Lee L and Kim J B 2008 *Opt. Express* **16** 12163

[18] Yang B D, Liang Q B, Zhang T C and Wang J M 2010 *Phys. Rev.* A **81** 043803

[19] Field J E, Hahn K H and Harris S E 1991 *Phys. Rev. Lett.* **67** 3062

[20] Moon H S, Lee L and Kim J B 2005 *J. Opt. Soc. Am.* B **22** 2529

[21] Wynands R and Nagel A 1999 *Appl. Phys.* B **68** 1

[22] Budker D, Yashchuk V and Zolotorev M 1998 *Phys. Rev. Lett.* **81** 5788

[23] Iftiquar S M, Karve G R and Natarajan V 2008 *Phys. Rev.* A **77** 063807

[24] Harris M L, Adams C S, Cornish S L, Mcleod I C, Tarleton E and Hughes I G 2006 *Phys. Rev.* A **73** 062509

[25] Yang B D, Zhao J Y, Zhang T C and Wang J M 2009 *J. Phys.* D: *Appl. Phys.* **42** 085111

[26] Moon H S, Lee W K, Lee L and Kim J B 2004 *Appl. Phys. Lett.* **85** 3965